Journal of Medicinal Chemistry

Article

pubs.acs.org/jmc

Synthesis and Biological Properties of Highly Sequence-Specific-Alkylating *N*-Methylpyrrole–*N*-Methylimidazole Polyamide Conjugates

Gengo Kashiwazaki,[†] Toshikazu Bando,*[,†] Tomofumi Yoshidome,[†] Seiji Masui,[†] Toshiki Takagaki,[†] Kaori Hashiya,[†] Ganesh N. Pandian,[‡] Junichi Yasuoka,[§] Kazunari Akiyoshi,[§,⊥] and Hiroshi Sugiyama*[,†,‡]

[†]Department of Chemistry, Graduate School of Science, Kyoto University, Kitashirakawa-oiwakecho, Sakyo-ku, Kyoto 606-8502

[‡]Institute for Integrated Cell-Material Sciences (iCeMS), Kyoto University, Yoshida-ushinomiyacho, Sakyo-ku, Kyoto 606-8501

[§]Institute of Biomaterials and Bioengineering, Tokyo Medical and Dental University, 2-3-10 Kanda-Surugadai, Chiyoda-ku, Tokyo 101-0062

[⊥]Graduate School of Engineering, Kyoto University, Kyoto daigaku-Katsura, Nishikyo-ku, Kyoto 615-8530

Supporting Information

ABSTRACT: Four new alkylating *N*-methylpyrrole-*N*-methylimidazole (PI) polyamide conjugates (**1**–**4**) with seven-base-pair (bp) recognition ability were synthesized. Evaluation of their DNA-alkylating activity clearly showed accurate alkylation at match site(s). The cytotoxicities of conjugates **1**–**4** were determined against six human cancer cell lines, and the effect of these conjugates on the expression levels of the whole human genome in A549 cells were also investigated. A few genes among the top 20 genes were commonly downregulated by each conjugate, which reflects their sequence specificity. Conversely, many of the top 10 genes were commonly upregulated, which may have been caused by alkylation damage to DNA. Moreover, the antitumor activities of the PI polyamide conjugates **2** and **3** were investigated using nude mice transplanted with DU145 or A549. The intravenous administration of each liposomal conjugate in water yielded tumor-suppressing effects specifically toward DU145 cells and not A549 cells, which was pertinent to cytotoxicity.

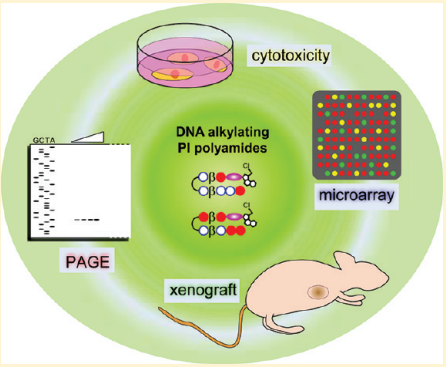

INTRODUCTION

DNA-alkylating agents can damage cellular DNA and may lead to anticancer activity.[1] However, the selectivity of these agents toward cancer cells over normal cells usually depends upon the rapid proliferation of cancer cells and severe side effects are caused by nonspecific DNA alkylation in normal cells. To address this issue, we exploited the sequence-recognizing ability of *N*-methylpyrrole–*N*-methylimidazole (PI) polyamides[2] to elucidate if the introduction of sequence-selectivity into DNA-targeting agents could improve their function as antitumor agents.[3] We used indole as a linker[4] between a PI polyamide moiety and 1-chloromethyl-5-hydroxy-1,2-dihydro-3*H*-benz[*e*]-indole (*seco*-CBI),[5] which alkylates the N3 position of adenine. These alkylating conjugates can alkylate DNA in an atom-specific manner and have strong cytotoxicity.[6] However, as cytotoxicity level alone is insufficient to provide informative indication of intracellular dynamics, gene expression patterns have been analyzed using the microarray technique: (i) HLC-2 cells treated with short alkylating PI polyamide conjugates possessing a vinyl linker and Du86,[7] (ii) MT2 cells treated with two PI polyamides,[8] (iii) SW620 cells treated with H4c-targeting chlorambucil conjugates,[9] (iv) RT4 cells treated with alkylating conjugates with a vinyl linker and Du86 to evaluate the effects of replacing P with I,[10] (v) Friedreich's ataxia cells treated with GAA-repeat-targeting and 1:1-binding PI polyamide,[11] (vi) K562 cells treated with alkylating conjugates with an indole linker and *seco*-CBI, as used in this study, to confirm the downregulation of H4-related genes,[3e] (vii) renal cortices from high-salt rats after intravenous administration of a PI polyamide targeting TGF-β1.[12] Herein, we examined the effects of four alkylating conjugates on the expression of the whole human genome (~25 000 genes).

Moreover, animal tests were performed to evaluate the in vivo antitumor activity of the conjugates toward xenografts of human cancer cell lines transplanted into nude mice. Several reports have described this application of PI polyamides to animal models: in xenograft studies using K562–chlorambucil conjugates,[13] in PET imaging,[14] for the suppression of metastasis via inhibition of MMP-9,[15] and for corneal wound healing after damage by alkali.[16] The in vivo anticancer activities of duocarmycin analogues against melanoma were also investigated.[17] However, the in vivo antitumor activities of alkylating PI polyamide conjugates possessing *seco*-CBI have

Received: September 20, 2011
Published: February 6, 2012

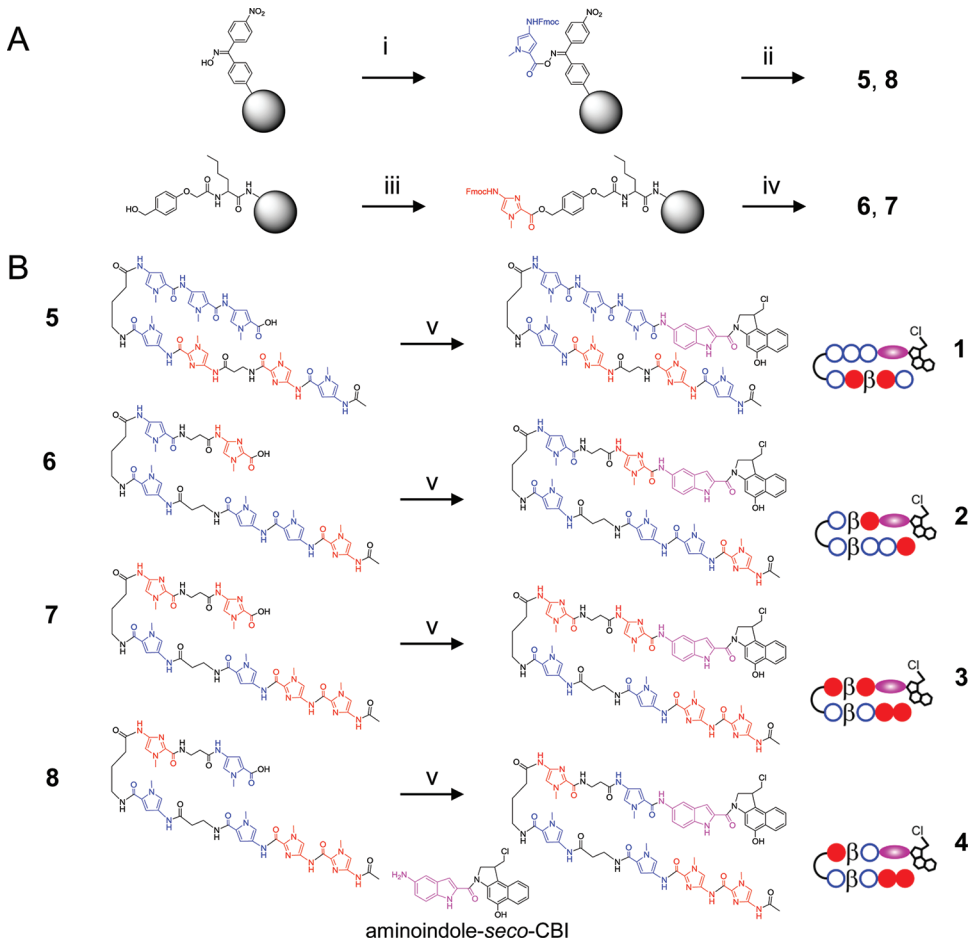

Figure 1. Synthetic scheme for the preparation of PI polyamide conjugates **1**-**4**: (A) Loading of Fmoc P/I monomer on oxime resin and CLEAR-Acid resin, respectively, and solid-phase peptide syntheses. (i) FmocNH-*N*-methylpyrrole-CO_2H, DCC, HOBt, DIEA; (ii) Fmoc solid-phase synthesis was followed by cleavage with 1 M NaOH in 1,4-dioxane, rt, 2 h; (iii) FmocNH-*N*-methylimidazole, MSNT, *N*-methylimidazole; (iv) Fmoc solid-phase synthesis was followed by cleavage with TFA; (B) (v) aminoindole−*seco*-CBI, PyBOP, DIEA in DMF, rt, overnight.

not been examined. Our strategy is to prepare and inject liposomal and naked conjugates into mouse xenograft models.

Liposomes are used extensively in molecular biology and medicine, partially because of the enhancement of the antitumor activity of natural agents, such as isoflavone and curcumin, afforded by these vesicles and because liposomal conjugates exhibit high bioavailability and faster and better absorption.[18] Moreover, it is also possible to prepare proteoliposomes by integrating cell-free-synthesized, water-insoluble membrane proteins into liposomes, without losing their function.[19]

Thus, we carried out the biological evaluation of alkylating PI polyamide conjugates containing *seco*-CBI. The results of the microarray analysis and the correlation of polyacrylamide gel electrophoresis (PAGE) results, cytotoxicity, and in vivo antitumor effects will be discussed.

RESULTS AND DISCUSSION

Design and Syntheses. Design of conjugates **1**−**4** was based on the evaluation of the alkylating functions of six other synthesized conjugates. Three 9-bp recognition conjugates (IIP-*β*-IPP-*γ*-IPP-*β*-P−indole−*seco*-CBI, IIP-*β*-IIP-*γ*-PPP-*β*-P−indole−*seco*-CBI, IPP-*β*-IIP-*γ*-IPP-*β*-P−indole−*seco*-CBI) and two 7-bp recognition conjugates (IIP-*β*-I-*γ*-P-*β*-P−indole−*seco*-CBI, IIP-*β*-I-*γ*-PPP−indole−*seco*-CBI) had insufficient sequence-specificity, and one 7-bp recognition conjugate (IIP-*β*-P-*γ*-IPP−indole−*seco*-CBI) had alkylating activity lower than that of conjugate **4** (the schematic representation is in Figure S1 in Supporting Information).

Four alkylating PI polyamide conjugates were synthesized to target 7-bp sequences. PI polyamide moieties **5** and **8** were synthesized on oxime resin, and moieties **6** and **7** were synthesized on CLEAR-Acid resin, using Fmoc solid-phase synthesis and were cleaved with sodium hydroxide and TFA, respectively, to yield each carboxylic acid (**5**−**8**). Subsequently, the aminoindole−*seco*-CBI was coupled with each carboxylic acid (**5**−**8**) in DMF using PyBOP and DIEA. The target products were used in PAGE, the cytotoxicity assay, and animal test evaluations after high performance liquid chromatography (HPLC) purification. The structures and synthetic schemes of the alkylating PI polyamide conjugates **1**−**4** are shown in Figure 1.

DNA-Alkylating Activity of Conjugates 1−4. The alkylating activities and sequence specificities of conjugates **1**−**4** were evaluated using PAGE. Alkylation was performed at room temperature for 12 h, followed by addition of calf thymus DNA. The samples were heated at 95 °C under neutral conditions for 5 min. Under these heating conditions, all N3 positions of adenines at the alkylated sites in the quantitative DNA fragments as cleavage bands were produced on the gel.

dx.doi.org/10.1021/jm201225z | *J. Med. Chem.* 2012, 55, 2057−2066

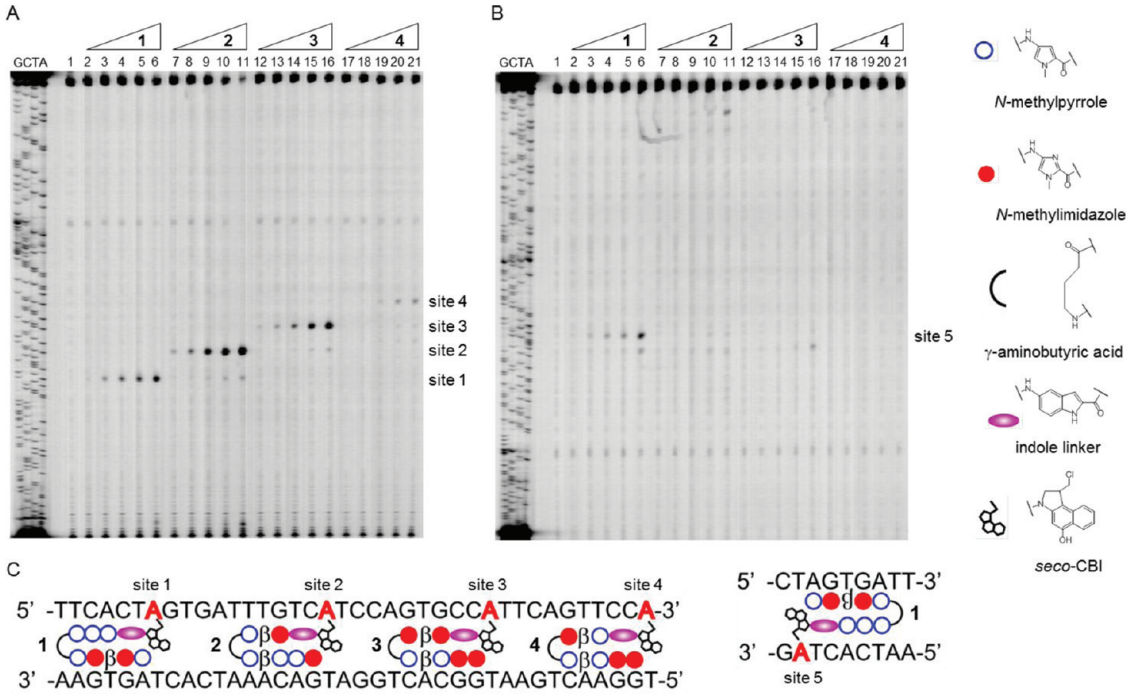

Figure 2. Thermally induced strand cleavage of the 5′-Texas Red-labeled 208-bp DNA fragment (6.0 nM) by conjugates **1**–**4** at rt for 12 h. Alkylation for the upper strand (see C) and for the lower strand are shown in A and B, respectively. Lane 1, DNA control; lanes 2–21, 10, 25, 50, 100, 200 nM of **1** (lanes 2–6), **2** (lanes 7–11), **3** (lanes 12–16), and **4** (lanes 17–21). (C) Schematic representations of adenine alkylations by each conjugate for both strands.

Table 1. Log IC_{50} Values of Conjugates 1–4 after Treatment for 48 h[a]

conjugate	DU145	A549	PC-3	EBC-1	SK-N-SH	K562
1	−8.48 ± 0.13	−7.67 ± 0.08	−8.22 ± 0.10	−7.47 ± 0.15	−7.82 ± 0.04	−8.11 ± 0.17
2	−8.22 ± 0.19	−7.59 ± 0.09	−7.90 ± 0.05	−7.22 ± 0.21	−7.72 ± 0.06	−8.04 ± 0.12
3	−8.20 ± 0.18	−7.47 ± 0.08	−7.72 ± 0.06	−6.77 ± 0.24	−7.39 ± 0.09	−7.94 ± 0.05
4	−7.95 ± 0.20	−7.00 ± 0.08	−7.53 ± 0.11	−6.26 ± 0.22	−6.89 ± 0.05	−7.81 ± 0.03

[a] n = 3 for DU145, A549, SK-N-SH, and n = 6 for PC-3 and EBC-1.

Figure 2 shows the results of PAGE using conjugates **1**–**4** and both sides of 208-bp PCR products. PI polyamide conjugates **1**, **2**, **3**, and **4** recognized 7-bp sequences and alkylated site 1 (5′-TTCACTA-3′), site 2 (5′-TTTGTCA-3′), site 3 (5′-AGTGCCA-3′), and site 4 (5′-AGTTCCA-3′) of the DNA fragment, respectively. In the complementary strand, conjugate **1** alone had one match site (site 5: 5′-ATCACTA-3′) and there were no match sites for conjugates **2**, **3**, and **4**. Conjugate **4** had a significantly lower alkylating activity, whereas conjugates **1**, **2**, and **3** produced alkylating bands, even at 10 or 25 nM. It is noteworthy that all four conjugates showed alkylating bands only at match site(s) and that these conjugates did not show any alkylating bands for mismatch sites, even when the substrate DNA contained several 1-bp mismatch sites: the upper strand (Figure 2A) contained 1, 2, 1, and 2 sites as 1-bp mismatch site(s), and the lower strand (Figure 2B) contained 5, 3, 1, and 0 sites as 1-bp mismatch site(s) for conjugates **1**, **2**, **3**, and **4**, respectively (the schematic representations are in Figure S2 in Supporting Information). Hence, these PAGE results clearly indicate that these four conjugates have high sequence specificity and that conjugates **2** and **3**, in particular, have alkylating activities.

Cytotoxicity of Conjugates 1–4 against Six Human Cancer Cell Lines. Next, we determined the IC_{50} values (the concentration that yields 50% cell-growth inhibition) against six human cancer cell lines: DU145, A549, PC-3, EBC-1, SK-N-SH, and K562 (Table 1). As is generally the case for PI polyamide conjugates possessing *seco*-CBI as an alkylating moiety, the IC_{50} values obtained here were as low as ∼50 nM against any of the cell lines. Among the cell lines tested, DU145 was the most sensitive and A549 was the second-least sensitive to all conjugates. The comparison of these IC_{50} values revealed that conjugates **1**, **2**, and **3** had lower values than conjugate **4**. It is important to note here that conjugates **1**, **2**, and **3** also had higher alkylating activity (Figure 2). Nevertheless, PAGE results alone may not predict cytotoxicity if the alkylating moiety conjugated to the PI polyamide changes from *seco*-CBI to chlorambucil.[3f]

Microarray Analysis. A549 cells were treated with each conjugate at the respective IC_{50} concentration for 12 h (21, 26, 34, and 100 nM for conjugates **1**, **2**, **3**, and **4**, respectively). Among ∼25 000 genes of the human genome, 302, 446, 517, and 849 genes were upregulated by more than 2-fold and 187, 196, 231, 1102 genes were more than 2-fold downregulated by conjugates **1**, **2**, **3**, and **4**, respectively. The top 20 down-regulated transcripts and top 10 upregulated transcripts were extracted for each conjugate, although, intriguingly, alkylating conjugates that were designed for gene silencing also upregulated many genes. Partial dependency on the concentrations of PI polyamide conjugates was observed. For

dx.doi.org/10.1021/jm201225z | J. Med. Chem. 2012, 55, 2057–2066

Table 2. Bottom 20 and Top 10 Gene Expressions after Treatment with Each Conjugate[a]

		conjugate 1		conjugate 2		conjugate 3		conjugate 4		
		name	fold	name	fold	name	fold	name	fold	
downregulation	1	RABGAP1L	0.132	DPYD	0.115	DPYD	0.103	PTPRK	0.026	2
	2	NP_115632.1	0.154	RABGAP1L	0.155	NBEA	0.152	FUT8	0.035	3
	3	Q8N570_HUMAN	0.228	RABGAP1L	0.215	Q8N570_HUMAN	0.186	RPS6KC1	0.038	4
	4	RS29_HUMAN	0.234	PTPRK	0.257	PTPRK	0.189	ELP4	0.045	
	5	FHIT	0.253	SLC4A4	0.273	SUPT3H	0.231	SUPT3H	0.052	
	6	SUPT3H	0.268	Q8N570_HUMAN	0.283	ZNF407	0.241	Q8TC78_HUMAN	0.056	
	7	NBEA	0.274	ACTG_HUMAN	0.311	Q9P223_HUMAN	0.258	EFA6R_HUMAN	0.058	
	8	SLC4A4	0.278	TNIK	0.312	NP_115632.1	0.273	NP_112224.1	0.058	
	9	MBD3L1	0.294	ADH1A	0.317	RABGAP1L	0.276	NP_653244.1	0.061	
	10	NP_060463.1	0.303	NP_940865.1	0.322	Q8NBA2_HUMAN	0.276	GULP1	0.062	
	11	CPNE4	0.314	Q5W0V6_HUMAN	0.324	SMYD3	0.291	SEMA3A	0.063	
	12	PTPRK	0.334	HS2ST1	0.329	LAMA2	0.300	PDE7B	0.064	
	13	GABRA3	0.343	MYCBP2	0.338	ACTG_HUMAN	0.307	UVRAG	0.066	
	14	FMN2	0.344	NBEA	0.339	GTDC1	0.307	XRCC4_HUMAN	0.067	
	15	ACTG_HUMAN	0.345	XP_375606.2	0.350	SIPA1L1	0.309	NP_060504.1	0.068	
	16	SMYD3	0.345	EPM2A	0.353	ZNF291	0.311	NCOA1_HUMAN	0.068	
	17	HECW2	0.346	SEMA3E	0.353	NP_001027.2	0.313	FAF1	0.071	
	18	Q8NCR4_HUMAN	0.348	Q9Y6Z5_HUMAN	0.356	GPX6	0.322	TCF12	0.074	
	19	Q5VY43_HUMAN	0.354	CTTNBP2	0.360	OR1C1	0.324	NP_056993.2	0.076	
	20	SLC25A21	0.354	HIST1H2AC	0.362	HIST1H2AC	0.329	DYM	0.080	
upregulation	1	HES2	10.6	SPESP1	11.0	BTG2	9.7	HES2	19.2	2
	2	Q6NTF7_HUMAN	7.0	BTG2	10.1	MDM2	8.9	MDM2	15.6	3
	3	BTG2	6.7	HES2	9.4	BBC3	8.5	BTG2	13.0	4
	4	BBC3	5.7	BBC3	9.4	HES2	8.2	RRAD	11.2	
	5	MDM2	5.4	CDKN1A	8.2	CDKN1A	7.8	BBC3	10.7	
	6	CST8	5.3	MDM2	8.1	GLS2	6.7	NPPC	10.5	
	7	CDKN1A	5.2	GADD45A	7.0	KRTHA4	6.1	U124_HUMAN	10.3	
	8	HCK	4.3	RRAD	6.0	NP_997213.1	6.0	CDKN1A	9.0	
	9	FDXR	2.0	PPM1D	5.7	GADD45A	5.9	GADD45A	8.3	
	10	BTNL3_HUMAN	2.0	GDF15	5.5	U124_HUMAN	5.6	FDXR	8.2	

[a]A549 cells were treated for 12 h at IC_{50} concentration, 21, 26, 34, and 100 nM of each conjugate **1**, **2**, **3**, and **4**. Overlapping numbers are indicated by darkness of blue or red.

conjugate **4**, with the highest inducing concentration, more upregulation and downregulation was observed than for the other three counterparts. Although there is a slight correlation on the downregulation side even among the other three conjugates **1**−**3**, arithmetic average of all the downregulated genes demonstrated this speculation to be incorrect: 0.844, 0.840, 0.846, 0.755 fold for conjugate **1**−**4**, respectively.

Overlapping genes for each conjugate are indicated by the shade of the blue color for downregulation and by the shade of the red color for upregulation (Table 2). For example, PTPRK was downregulated by all four conjugates, SUPT3H was downregulated by three conjugates **1**, **3**, and **4**, NP_115632.1 was downregulated by two conjugates **1** and **3**, and RS29_HUMAN was downregulated by one conjugate **1**. The Ensembl ID and description of the genes are provided in Table S2 in the Supporting Information.

We found that 1, 5, 5, and 51 out of 62 genes appeared on the downregulation side in four, three, two, and one group, respectively. These relatively low ratios of shared genes may indicate that downregulation of a subset of genes examined was a primary consequence of PI polyamide sequences, although the number of alkylation sites for each conjugate did not explain the expression levels, as discussed previously in several papers.[3e,10] In other words, more match sites of an alkylating conjugate in the DNA sequence of a certain gene do not necessarily result in lower expression of that gene. Additionally it was found that the RTPRK gene involved in growth control and metastasis was downregulated commonly when A549 was treated with conjugate **2** or **3**, conjugates which were also used in the next animal tests. This kind of downregulation might contribute to in vitro and/or in vivo antitumor activities.

In contrast, 5, 1, 3, and 11 out of 20 genes appeared on the upregulation side in four, three, two, and one group, respectively. Interestingly, these common genes included the Bcl-2-binding component 3 (BBC3), which induces apoptosis, the antiproliferative protein BTG2, the cyclin-dependent kinase inhibitor 1 (p21, CDKN1A), and the growth-arrest and DNA-damage-inducible protein GADD45A. These "nonspecific" upregulations can be considered as general and indirect responses to alkylation by the conjugates, rather than a specific response of the alkylated gene. The conclusion that more genes were shared on the upregulation side does not change even after expanding the target genes by four times: top 80 and 40 for downregulation and upregulation sides, respectively (Table S1 in Supporting Information). Hierarchical clustering of genes that were within the top 800 of upregulation or downregulation sides by treatment with either of the alkylating PI polyamide conjugates **1**−**4** (Figure S3 in Supporting Information). This heat map again emphasized that conjugate **4** induced distinct downregulation levels and showed that there were few genes that are oppositely regulated by either two conjugates. Pathway analysis extracted the pathways which had a significantly higher density of upregulated genes by each conjugate (Table S3 and Figure S4 in Supporting Information). Interestingly, an apoptosis pathway emerged equally out of 5, 3, 5, and 2 pathways that were screened for conjugates **1**−**4**, respectively, due to irregular upregulation (Table S3 in Supporting Information). This analysis corroborates our hypothesis that the genes on the upregulation side are attributed to general responses toward alkylation.

Animal Tests. On the basis of IC_{50} values (Table 1), DU145 and A549 cells were chosen to evaluate the in vivo

dx.doi.org/10.1021/jm201225z | J. Med. Chem. 2012, 55, 2057−2066

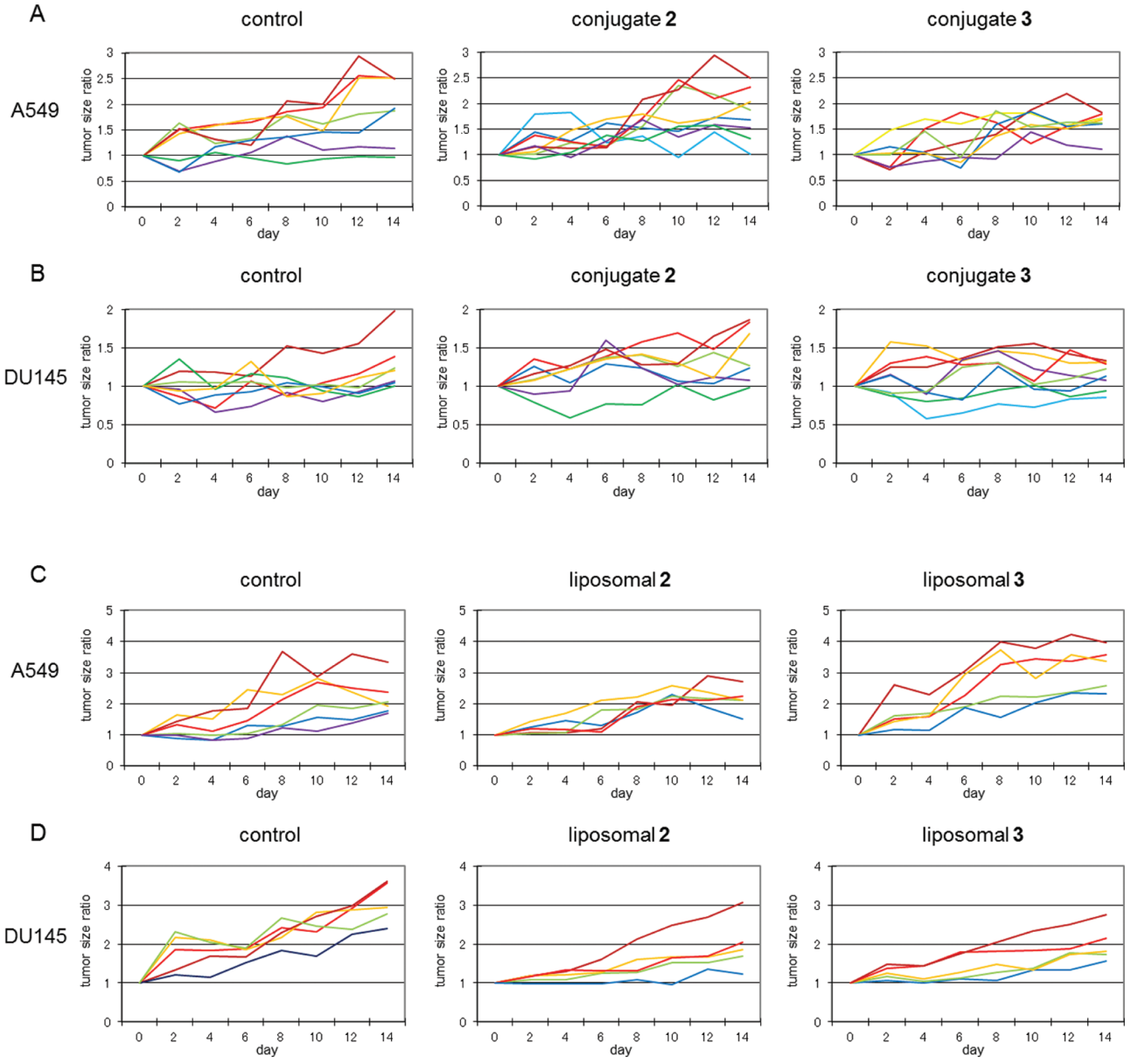

Figure 3. Profiles of tumor size ratios of nude mice transplanted with A549 or DU145 and treated with naked/liposomal conjugates **2** or **3** at day 0 (n = 7 or 8 for naked conjugates, and n = 5 or 6 for liposomal conjugates). Conjugate solutions were 20 μL at 625 μg/mL for naked conjugates **2** and **3**, and 125 μL at 330 μg/mL for liposomal conjugates **2** and **3**. The naked conjugates and the liposomal conjugates were injected intraperitoneally and intravenously, respectively. (A) A549 mice: control, naked conjugate **2**, and naked conjugate **3**. (B) DU145 mice: control, naked conjugate **2**, and naked conjugate **3**. (C) A549 mice: control, liposomal conjugate **2**, and liposomal conjugate **3**. (D) DU145 mice: control, liposomal conjugate **2**, and liposomal conjugate **3**.

antitumor activity of conjugates **2** and **3**, as the large difference in cytotoxicity of these cells was expected to contribute to a possible correlation between cytotoxicity and in vivo antitumor activity. Conjugates **2** and **3** were used in these tests owing to their high sequence specificity and alkylating activity (Figure 2) and because this conjugate combination possesses the largest difference in *N*-methylimidazole content. Tumor size and weight were measured every other day for 14 days (Tables S4–S11 in Supporting Information).

In the first animal test, naked conjugate solutions were injected intraperitoneally into xenografted mice. Because of the poor solubility of these conjugates in water, 100% DMSO was used to prepare solutions, which means intravenous administration was not applicable. However, almost no tumor-suppressing effects were observed under these conditions (Figure 3, conjugates **2** and **3**, A549, and DU145).

Therefore, liposomes were used to encapsulate conjugates **2** and **3** for the second animal test. The concentration of liposomal conjugates **2** and **3** was 330 μg/mL in 17 mM lipid, and 125 μL of each solution was administered intravenously to nude mice with DU145 or A549 xenografts, exclusively on the first day of the experiment (Figure 3, liposomal conjugates **2** and **3**, A549, and DU145). In A549-xenografted mice, neither of the liposomal conjugates **2** or **3** showed any tumor-suppressing effects. In DU145-xenografted mice, in contrast, liposomal conjugate **2** exhibited antitumor activity.

This difference in antitumor activities against DU145- and A549-xenografted mice may be attributed to cellular properties

dx.doi.org/10.1021/jm201225z | *J. Med. Chem.* 2012, 55, 2057–2066

or environmental factors specific to each cell line. The naked and liposomal conjugates also showed different antitumor activities. This difference may be explained by (i) the amount of conjugates injected into mice: 12.5 μg/mouse or 0.50 mg/kg for mice weighing 25 g in the case of naked conjugates, and 41 μg/mouse or 1.6 mg/kg in the case of liposomal conjugates; (ii) the administration routes: intraperitoneal for naked conjugates and intravenous for liposomal conjugates; (iii) the timing of conjugate administration: earlier for the tests of liposomal conjugates than for the tests of naked conjugates; as alkylating PI polyamide conjugates were not antiangiogenic but were expected to block cell growth by damaging DNA, injection at an earlier stage should be more effective; and (iv) liposomal effects: enhanced permeability and retention (EPR) effects,[20] for example. We pre-examined the toxicity of the naked and liposomal conjugate **2** against nude mice without xenografts. While an intraperitoneal dose of 0.50 mg/kg naked conjugate **2** was barely tolerated, an intravenous dose of 1.6 mg/kg of liposomal conjugate **2** did not yield toxicity. However, this 1.6 mg/kg dose was nearly the maximum possible concentration that could be prepared.

In anticancer therapeutics, studies on the genes that are responsible for each cancer is under vigorous study, and validity of a "one-target gene" strategy is disputed. Combination of alkylating PI polyamide conjugates could be developed as an optimal strategy to reveal the specific set of genes that actually correspond to a specific type of cancer. Not just polyamide design based on the available sequence of some target gene but also the screening of the conjugate library can be effective. Regarding the rational way to improve our compound, gene regulation by pyrrole−imidazole polyamides has been rapidly advancing. Potential strategies that could be used to improve biological functions of alkylating PI polyamide conjugates are as follows: (i) considering that *R-seco*-CBI has no alkylating activity,[21] chiral *S-seco*-CBI can be used instead of the racemic-*seco*-CBI, which has been used in this paper; (ii) employment of a vinyl linker instead of an indole linker for higher alkylating activity, which is obvious from comparison of reaction time;[4,21] (iii) increase in the recognition of the target DNA sequence.

CONCLUSIONS

Four alkylating PI polyamide conjugates were synthesized, and their sequence specificity was validated using PAGE analysis. Among the six human cancer cell lines for which IC_{50} values were determined, two cell lines, DU145 and A549, were transplanted into nude mice and the in vivo antitumor activity of two conjugates (**2** and **3**) was evaluated in the presence and absence of liposomes. The results indicate that liposomes are a good carrier for these conjugates. The results of a microarray analysis of the whole human genome suggest that the genes that were downregulated reflect the sequence specificity of conjugates, and that the genes that were upregulated reflect "nonspecific" alkylation by conjugates, because they included characteristic genes shared by all the conjugate-treated groups, such as apoptosis-promoting protein, antiproliferative protein, p21, and the growth-arrest and DNA-damage-inducible protein.

EXPERIMENTAL SECTION

General Remarks. Reagents and solvents were purchased from standard suppliers and used without further purification. Water (18 MΩ) was purified with a Millipore Milli-Q purification system. NMR spectra were recorded with a JEOL JNM-FX 400 nuclear magnetic resonance spectrometer, and tetramethylsilane was used as the internal standard. ^{1}H NMR spectra were recorded in parts per million (ppm) downfield relative to tetramethylsilane. The following abbreviations apply to spin multiplicity: s (singlet), d (doublet), t (triplet), brt (broad triplet), m (multiplet).

Purity of Final Compounds. Conjugates **1**−**4** were estimated to have a purity of higher than or equal to 95% based on HPLC and electrospray ionization mass spectrometry (ESI-TOFMS) analysis. The HPLC system for these analyses encompasses a PU-2080 Plus pump, a UV-2075 Plus UV/vis detector, a MX-2080-32, a DG-2080-54 degasser, and a CO-2060 Plus thermostat. The column was 4.6 mm × 150 mm and was filled with Chemcobond 5-ODS-H (Chemco Scientific Co., Ltd.). Gradient elution was employed wherein acetonitrile−0.1% AcOH water ratio was increased linearly from 0% to 100% acetonitrile over 20 min at a flow rate of 1.0 mL/min at 40 °C. ESI-TOFMS was obtained on a BioTOF II (Bruker Daltonics) mass spectrometer. Compound purities were determined by integrating peak areas of HPLC charts.

Preparation of P/I-Loaded Resin. Preparation of FmocNH-*N*-methylimidazole-loaded CLEAR-Acid resin is as follows: CLEAR-Acid resin (Peptides International Inc., ∼2 g) was swollen in DMF in Big LibraTube (HiPep Laboratories). FmocNH-*N*-methylimidazole-CO_2H (3.0 equiv), MSNT (3.0 equiv), and *N*-methylimidazole (8.0 equiv) were dissolved in dichloromethane and DMF, but a transparent solution is not required. The resin in this coupling mixture was shaken overnight, filtered, and washed with DMF, MeOH, and dichloromethane. Subsequently, the resin was treated with 20% Ac_2O in DMF for 1 h and washed with DMF and dichloromethane. Quantification was as previously reported.[3d] Preparation of Fmoc-*N*-methylpyrrole-loaded oxime resin is as follows: oxime resin (Wako, ∼2 g) was swollen in DMF in BigLibra Tube. FmocNH-*N*-methylpyrrole-CO_2H (4.0 equiv), DCC (4.0 equiv), HOBt (4.0 equiv), and DIEA (7.0 equiv) were dissolved in DMF. The resin in this coupling mixture was shaken overnight. Subsequent treatment is the same as for FmocNH-*N*-methylimidazole-loaded CLEAR-Acid resin.

Solid-Phase Machine-Assisted Synthesis of PI Polyamides. Syntheses of PI polyamides were assisted by a peptide synthesizer, PSSM-8 (Shimadzu). Procedures were as follows: swelling of resin (P-oxime resin/I-CLEAR-Acid resin) (80 mg) with DMF; deprotection by 20% piperidine in DMF for 4 min twice; removal of the solution, wash with DMF, and N_2 bubbling for 1 min five times; coupling by adding monomer units (4.0 equiv), HCTU (4.0 equiv), and DIEA (4.0 equiv) in NMP and N_2 bubbling for 30 min; removal of the solution, wash with DMF, and N_2 bubbling for 1 min five times. After the last coupling cycle, deprotected amino group was acetylated with 20% Ac_2O in DMF.

Determination of Concentrations of PI Polyamide Conjugates. Molar extinction coefficients ε of PI polyamides in DMF solution at around 305 nm were calculated as follows:

$$\varepsilon = 9900 \times (\text{number of P and I})$$

For indole−*seco*-CBI PI polyamide conjugates, 17 000 was added to the ε calculated above. Concentrations of PI polyamides were determined by the Lambert−Beer law.

$$\text{Abs} = \varepsilon c l$$

where Abs, c, and l are absorbance, molar concentration, and the path length, respectively. A NanoDrop 1000 spectrophotometer (Thermo Fisher Scientific Inc.) was used for measuring absorbance.

AcPI-*β*-IP-*γ*-PPP-CO_2H (5). After synthesis of AcPI-*β*-IP-*γ*-PPP-oxime resin in a stepwise reaction by the Fmoc solid-phase protocol (vide ante), the resin was treated with 500 μL of 2 M NaOH and 500 μL of 1,4-dioxane at 55 °C for 2 h. After filtration, the filtrate was quenched with HCl_{aq} and recrystallized from and washed with Et_2O. The retention time of compound **5** was 12.4 min (0.1% AcOH containing 0−100% acetonitrile over a linear gradient for 20 min at a flow rate of 1.0 mL/min at 40 °C detected at 254 nm). ESI-TOFMS m/z calcd for $C_{49}H_{57}N_{18}O_{11}$ $[M + H]^+$ 1073.45, found 1073.44. ^{1}H NMR (400 MHz, DMSO-d_6) 10.36 (s, 1H; I/P-amide), 10.32 (s, 1H; I/P-amide), 9.90 (s, 2H; I/P-amide), 9.88 (s, 1H; I/P-amide), 9.83 (s, 1H; I/P-amide), 9.80 (s, 1H; I/P-amide), 8.06 (t, J = 6.0 Hz, 1H; *β*/*γ*-

alanine-amide), 7.89 (t, J = 5.6 Hz, 1H; β/γ-alanine-amide), 7.50 (s, 1H; I-H), 7.45 (s, 1H; I-H), 7.41 (s, 1H; P-H), 7.23 (s, 2H; P-H), 7.21 (s, 1H; P-H), 7.17 (s, 1H; P-H), 7.04 (s, 1H; P-H), 6.96 (s, 1H; P-H), 6.90 (s, 1H; P-H), 6.86 (s, 1H; P-H), 6.83 (s, 1H; P-H), 3.95 (s, 3H; I-NMe), 3.94 (s, 3H; I-NMe), 3.84 (s, 3H; P-NMe), 3.83 (s, 3H; P-NMe), 3.82 (s, 3H; P-NMe), 3.82 (s, 3H; P-NMe), 3.81 (s, 3H; P-NMe), 3.53 (t, J = 5.6 Hz, 2H; methylene), 3.21 (m, 2H; methylene), 2.62 (t, J = 6.0 Hz, 2H; methylene), 2.28 (t, J = 7.2 Hz, 2H; methylene), 1.96 (s, 3H; Ac), 1.79 (t, J = 6.8 Hz, 2H; methylene).

AcIPP-β-P-γ-P-β-I-CO_2H (6). After synthesis of AcIPP-β-P-γ-P-β-I-CLEAR-Acid resin in a stepwise reaction by the Fmoc solid-phase protocol (vide ante), the resin was treated with 1 mL of TFA/TIS/water (95/2.5/2.5) at rt for 30 min. After filtration, the filtrate was recrystallized from and washed with Et_2O. The retention time of compound **6** was 11.1 min (0.1% AcOH containing 0−100% acetonitrile over a linear gradient for 20 min at a flow rate of 1.0 mL/min at 40 °C detected at 254 nm). ESI-TOFMS m/z calcd for $C_{46}H_{56}N_{17}O_{11}$ $[M + H]^+$ 1022.43, found 1022.43. ^{1}H NMR (400 MHz, DMSO-d_6) 10.55 (s, 1H; I/P-amide), 10.22 (s, 1H; I/P-amide), 9.94 (s, 1H; I/P-amide), 9.89 (s, 1H; I/P-amide), 9.83 (s, 1H; I/P-amide), 9.75 (s, 1H; I/P-amide), 8.02 (m, 3H; β/γ-alanine-amide), 7.48 (s, 1H; I-H), 7.42 (s, 1H; I-H), 7.26 (d, J = 2.0 Hz, 1H; P-H), 7.19 (d, J = 2.0 Hz, 1H; P-H), 7.12 (m, 2H; P-H), 7.10 (d, J = 2.0 Hz, 1H; P-H), 6.84 (s, 1H; P-H), 6.69 (s, 1H; P-H), 6.63 (s, 1H; P-H), 3.95 (s, 3H; I-NMe), 3.89 (s, 3H; I-NMe), 3.85 (s, 3H; P-NMe), 3.81 (s, 3H; P-NMe), 3.78 (s, 3H; P-NMe), 3.77 (s, 3H; P-NMe), 3.42 (m, 2H; methylene), 3.39 (m, 2H; methylene), 3.37 (m, 2H; methylene), 3.17 (t, J = 6.4 Hz, 2H; methylene), 2.52 (m, 2H; methylene), 2.24 (t, J = 8.0 Hz, 2H; methylene), 2.02 (s, 3H; Ac), 1.75 (t, J = 7.2 Hz, 2H; methylene).

AcIIP-β-P-γ-I-β-I-CO_2H (7). After synthesis of AcIIP-β-P-γ-I-β-I-CLEAR-Acid resin in a stepwise reaction by the Fmoc solid-phase protocol (vide ante), the resin was treated with 1 mL of TFA/TIS/water (95/2.5/2.5) at rt for 30 min. After filtration, the filtrate was recrystallized from and washed with Et_2O. The retention time of compound **7** was 11.3 min (0.1% AcOH containing 0−100% acetonitrile over a linear gradient for 20 min at a flow rate of 1.0 mL/min at 40 °C detected at 254 nm). ESI-TOFMS m/z calcd for $C_{44}H_{54}N_{19}O_{11}$ $[M + H]^+$ 1024.43, found 1024.43. ^{1}H NMR (400 MHz, DMSO-d_6) 10.59 (s, 1H; I/P-amide), 10.30 (s, 2H; I/P-amide), 10.26 (s, 1H; I/P-amide), 9.85 (s, 1H; I/P-amide), 9.33 (s, 1H; I/P-amide), 8.08 (t, J = 5.6 Hz, 1H; β/γ-alanine-amide), 7.99 (t, J = 8.0 Hz, 1H; β/γ-alanine-amide), 7.85 (t, J = 8.0 Hz, 1H; β/γ-alanine-amide), 7.56 (s, 1H; I-H), 7.50 (s, 1H; I-H), 7.44 (s, 1H; I-H), 7.39 (s, 1H; I-H), 7.23 (s, 1H; P-H), 7.11 (s, 1H; P-H), 6.95 (s, 1H; P-H), 6.67 (s, 1H; P-H), 3.99 (s, 3H; I-NMe), 3.98 (s, 3H; I-NMe), 3.90 (s, 3H; I-NMe), 3.89 (s, 3H; I-NMe), 3.81 (s, 3H; P-NMe), 3.77 (s, 3H; P-NMe), 3.50 (m, 2H; methylene), 3.43 (m, 2H; methylene), 3.37 (m, 2H; methylene), 3.15 (t, J = 6.0 Hz, 2H; methylene), 2.55 (m, 2H; methylene), 2.30 (t, J = 7.2 Hz, 2H; methylene), 2.04 (s, 3H; Ac), 1.75 (t, J = 7.2 Hz, 2H; methylene).

AcIIP-β-P-γ-I-β-P-CO_2H (8). After synthesis of AcIIP-β-P-γ-I-β-P-oxime resin in a stepwise reaction by Fmoc solid-phase protocol (vide ante), the resin was treated with 500 μL of 2 M NaOH and 500 μL of 1,4-dioxane at 55 °C for 2 h. After filtration, the filtrate was quenched with HCl_{aq} and recrystallized from and washed with Et_2O. The retention time of compound **8** was 12.0 min (0.1% AcOH containing 0−100% acetonitrile over a linear gradient for 20 min at a flow rate of 1.0 mL/min at 40 °C detected at 254 nm). ESI-TOFMS m/z calcd for $C_{45}H_{55}N_{18}O_{11}$ $[M + H]^+$ 1023.43, found 1023.43. ^{1}H NMR (400 MHz, DMSO-d_6) 10.32 (s, 1H; I/P-amide), 10.31 (s, 1H; I/P-amide), 10.27 (s, 1H; I/P-amide), 9.93 (s, 1H; I/P-amide), 9.84 (s, 1H; I/P-amide), 9.32 (s, 1H; I/P-amide), 8.09 (brt, 1H; β/γ-alanine-amide), 8.00 (brt, 1H; β/γ-alanine-amide), 7.92 (brt, 1H; β/γ-alanine-amide), 7.56 (s, 1H; I-H), 7.51 (s, 1H; I-H), 7.39 (s, 1H; I-H), 7.27 (d, J = 1.6 Hz, 1H; P-H), 7.23 (d, J = 1.6 Hz, 1H; P-H), 7.11 (d, J = 2.0 Hz, 1H; P-H), 6.96 (d, J = 1.6 Hz, 1H; P-H), 6.68 (d, J = 2.0 Hz, 1H; P-H), 6.67 (d, J = 2.0 Hz, 1H; P-H), 3.99 (s, 3H; I-NMe), 3.98 (s, 3H; I-NMe), 3.91 (s, 3H; I-NMe), 3.81 (s, 3H; P-NMe), 3.79 (s, 3H; P-NMe), 3.77 (s, 3H; P-NMe), 3.50 (m, 2H; methylene), 3.43 (m, 2H; methylene), 3.29(m, 2H; methylene), 3.15 (m, 2H; methylene), 2.54 (m, 2H; methylene), 2.31 (m, 2H; methylene), 2.04 (s, 3H; Ac), 1.75 (m, 2H; methylene).

Aminoindole−*seco*-CBI. This compound was synthesized as previously reported.[5c,22]

*AcPI-β-IP-γ-PPP−indole−seco-CBI (**1**).* To a solution of compound **5** (2.0 mg, 1.9 μmol) in DMF were added H_2N-indole−*seco*-CBI (1.0 equiv), PyBOP (3.0 equiv), and DIEA (6.0 equiv), and the solution was shaken at rt overnight. The solvent was removed, recrystallized from Et_2O, and purified by HPLC to obtain **1** (1.3 mg, 0.90 μmol, 47%). The retention time of compound **1** was 15.9 min (0.1% AcOH containing 0−100% acetonitrile over a linear gradient for 20 min at a flow rate of 1.0 mL/min at 40 °C detected at 254 nm). ESI-TOFMS m/z calcd for $C_{71}H_{73}ClN_{21}O_{12}$ $[M + H]^+$ 1446.54, found 1446.56. ^{1}H NMR (400 MHz, DMSO-d_6) 11.66 (s, 1H), 10.43 (s, 1H), 10.35 (s, 1H), 10.32 (s, 1H), 9.96 (s, 1H), 9.91 (s, 1H), 9.89 (s, 1H), 9.83 (s, 2H), 9.80 (s, 1H), 8.12 (m, 1H), 8.06 (brt, 1H), 7.97 (s, 1H), 7.90−7.85 (2H), 7.56−7.35 (8 H), 7.30 (s, 1H), 7.24 (s, 1H), 7.23 (d, J = 2.0 Hz, 1H), 7.21 (s, 1H), 7.17 (s, 1H), 7.14 (s, 1H), 7.08 (s, 1H), 6.96 (s, 1H), 6.90 (d, J = 2.0 Hz, 1H), 6.88 (d, J = 2.0 Hz, 1H), 4.81 (t, J = 10 Hz, 1H), 4.57 (d, J = 10.8 Hz, 1H), 4.23 (brt, 1H), 3.95−3.81 (23H), 3.53 (m, 2H), 3.38 (m, 2H), 3.21 (m, 2H), 2.52 (m, 2H), 1.96 (s, 3H), 1.79 (m, 2H).

*AcIPP-β-P-γ-P-β-I−indole−seco-CBI (**2**).* To a solution of compound **6** (10.0 mg, 9.8 μmol) in DMF were added H_2N-indole−*seco*-CBI (1.0 equiv), PyBOP (1.2 equiv), and DIEA (2.3 equiv), and the solution was shaken at rt overnight. The solvent was removed, recrystallized from Et_2O, and purified by HPLC to obtain **2** (3.9 mg, 2.8 μmol, 29%). The retention time of compound **2** was 15.3 min (0.1% AcOH containing 0−100% acetonitrile over a linear gradient for 20 min at a flow rate of 1.0 mL/min at 40 °C detected at 254 nm). ESI-TOFMS m/z calcd for $C_{68}H_{72}ClN_{20}O_{12}$ $[M + H]^+$ 1395.53, found 1395.52. ^{1}H NMR (400 MHz, DMSO-d_6) 11.72 (s, 1H), 10.44 (s, 1H), 10.42 (s, 1H), 10.23 (s, 1H), 9.95 (s, 1H), 9.89 (s, 1H), 9.83 (s, 1H), 9.78 (s, 1H), 9.76 (s, 1H), 8.13 (s, 1H), 8.05 (m, 3H), 7.97 (s, 1H), 7.86 (d, J = 8.4 Hz, 1H), 7.55−7.35 (8H), 7.23 (s, 1H), 7.19 (s, 2H), 7.12 (s, 1H), 7.11 (s, 1H), 6.84 (s, 1H), 6.69 (s, 1H), 6.66 (s, 1H), 4.81 (t, J = 10 Hz, 1H), 4.56 (d, J = 11.6 Hz, 1H), 4.24 (brt, 1H), 4.04 (m, 1H), 3.99 (s, 3H), 3.94 (s, 3H), 3.90 (m, 1H), 3.84 (s, 3H), 3.81 (s, 3H), 3.78 (s, 3H), 3.77 (s, 3H), 3.44 (m, 4H), 3.18 (m, 2H), 2.58 (t, J = 7.2 Hz, 2H), 2.42 (m, 2H), 2.24 (t, J = 7.6 Hz, 2H), 2.02 (s, 3H), 1.76 (m, 2H).

*AcIIP-β-P-γ-I-β-I−indole−seco-CBI (**3**).* To a solution of compound **7** (10.0 mg, 9.8 μmol) in DMF were added aminoindole−*seco*-CBI (1.0 equiv), PyBOP (1.2 equiv), and DIEA (2.3 equiv), and the solution was shaken at rt overnight. The solvent was removed, recrystallized from Et_2O, and purified by HPLC to obtain **3** (4.0 mg, 2.9 μmol, 29%). The retention time of compound **3** was 15.4 min (0.1% AcOH containing 0−100% acetonitrile over a linear gradient for 20 min at a flow rate of 1.0 mL/min at 40 °C detected at 254 nm). ESI-TOFMS m/z calcd for $C_{66}H_{70}ClN_{22}O_{12}$ $[M + H]^+$ 1397.52, found 1397.54. ^{1}H NMR (400 MHz, DMSO-d_6) 11.72 (s, 1H), 10.49 (s, 1H), 10.44 (s, 1H), 10.32 (s, 1H), 10.30 (s, 1H), 10.26 (s, 1H), 9.83 (s, 1H), 9.77 (s, 1H), 9.33 (s, 1H), 8.13−7.85 (7H), 7.56−7.37 (8H), 7.23 (s, 1H), 7.19 (s, 1H), 7.11 (s, 1H), 6.95 (s, 1H), 6.68 (s, 1H), 4.81 (t, J = 9.6 Hz, 1H), 4.56 (d, J = 12 Hz, 1H), 4.23 (brt, 1H), 3.99−3.77 (20H), 3.52 (m, 2H), 3.43 (m, 2H), 3.35 (m, 2H), 3.17 (m, 2H), 2.62 (m, 2H), 2.31 (m, 2H), 2.04 (s, 3H), 1.75 (m, 2H).

*AcIIP-β-P-γ-I-β-P−indole−seco-CBI (**4**).* To a solution of compound **8** (7.5 mg, 7.3 μmol) in DMF were added H_2N-indole−*seco*-CBI (1.0 equiv), PyBOP (3.0 equiv), and DIEA (6.0 equiv), and the solution was shaken at rt overnight. The solvent was removed, recrystallized from Et_2O, and purified by HPLC to obtain **4** (1.4 mg, 1.0 μmol, 14%). The retention time of compound **4** was 15.3 min (0.1% AcOH containing 0−100% acetonitrile over a linear gradient for 20 min at a flow rate of 1.0 mL/min at 40 °C detected at 254 nm). ESI-TOFMS m/z calcd for $C_{67}H_{71}ClN_{21}O_{12}$ $[M + H]^+$ 1396.53, found 1396.53. ^{1}H NMR (400 MHz, DMSO-d_6) 11.67 (s, 1H), 10.43 (s, 1H), 10.32 (s, 1H), 10.30 (s, 1H), 10.26 (s, 1H), 9.97 (s, 1H), 9.83 (s, 1H), 9.78 (s, 1H), 9.32 (s, 1H), 8.12 (d, J = 8.8 Hz, 1H), 8.07 (brt, 2H), 7.99−7.93

dx.doi.org/10.1021/jm201225z | J. Med. Chem. 2012, 55, 2057−2066

(3H), 7.86 (d, J = 8.4 Hz, 1H), 7.56−7.50 (4H), 7.44−7.37 (3H), 7.23 (s, 2H), 7.17 (d, J = 2.0 Hz, 1H), 7.11 (d, J = 2.0 Hz, 1H), 6.96 (d, J = 2.0 Hz, 1H), 6.94 (d, J = 2.0 Hz, 1H), 6.68 (d, J = 2.0 Hz, 1H), 4.81 (t, J = 10.0 Hz, 1H), 4.56 (d, J = 12.4 Hz, 1H), 4.23 (brt, 1H), 4.03−3.76 (20H), 3.53 (m, 2H), 3.44 (m, 2H), 3.16 (m, 2H), 2.57 (m, 2H), 2.33 (m, 4H), 2.04 (s, 3H), 1.75 (d, J = 7.0 Hz, 2H).

Preparation of 5′ Texas Red-Labeled 208-bp DNA Fragments. All DNA fragments and primers were purchased from Sigma-Aldrich. Two DNA fragments were annealed in a final volume of 20 μL containing 50 μM of each strand (5′-TGTCATCCAGTGCCATTCAGTTC-CATCCAGA-3′ and 5′-CTGGATGGAACTGAATGGCACTGGAT-GACAA-3′) and ligated into pGEM-T Easy vector (Promega). *Escherichia coli* DH5α competent cells were transformed and cultured on an LB plate with 100 μg/mL ampicillin, 25 μL of X-gal at 20 mg/mL, and 25 μL of IPTG at 100 mM overnight at 37 °C. White colonies were identified by colony PCR in 20 μL of the reaction mixtures containing 250 nM of each primer (SP6 primer: 5′-TATTTAGGT-GACACTATAG-3′, T7 primer: 5′-TAATACGACTCACTATAGGG-3′), 200 μM of dNTPs (Sigma-Aldrich), 2 units of Taq polymerase, and 1x ThermoPol reaction buffer (New England Bio Laboratories). Amplification cycles were carried out with an iCycler (Bio-Rad). The reaction mix was incubated at 95 °C for 5 min, followed by 35 cycles of 95 °C for 30 s, 50 °C for 30 s, 72 °C for 30 s, with a final extension step of 72 °C for 7 min. The insertion-confirmed colony was selected for transfer to 5 mL of LB medium with 100 μg/mL ampicillin and cultured overnight at 37 °C. The plasmid was extracted using GenElute Plasmid Miniprep Kit (Sigma-Aldrich). PCR condition from this inserted pGEM-T Easy vector: 95 °C for 5 min, followed by 35 cycles of 95 °C for 35 s, 50 °C for 35 s, 72 °C for 30 s, with a final extension step of 72 °C for 7 min. The fragment was purified by GenElute PCR cleanup kit (Sigma-Aldrich). The sequence of this PCR product (208 bp, the upper strand of Figure 2C) when 5′-Texas Red-labeled SP6 primer and T7 primer were used is 5′-TATTTAGGTGA-CACTATAGAATACTCAAGCTATGCATCCAACGCGTTGG-GAGCTCTCCCATATGGTCGACCTGCAGGCGGCCGCGAATT-CACTAGTGATTTGTCATCCAGTGCCATTCAGTTCCATCCA-GAATCGAATTCCCGCGGCCGCCATGGCGGCCGGGAG-CATGCGACGTCGGGCCCAATTCGCCCTATAGTGAGTCG-TATTA-3′. The complementary fragment (208 bp, the lower strand of Figure 2C) was obtained by PCR using 5′-Texas Red-labeled T7 primer and SP6 primer.

PAGE. The 5′-Texas Red-labeled DNA fragments were alkylated by alkylating polyamide conjugates **5**−**8** in 10 μL of 5.0 mM sodium phosphate buffer (pH 7.0) containing 10% DMF at room temperature for 12 h. The reaction was quenched by adding calf thymus DNA (10 mg/mL, 1 μL) and heated at 95 °C for 5 min. The DNA was recovered by centrifugal concentrator (TAITEC). The pellet was dissolved in 6 μL of loading dye (contents: 10 mL of formamide, 200 μL of water, 300 μL of 0.5 M aqueous solution of disodium dihydrogen ethylenediaminetetraacetate dihydrate, and 2.5 mg of New fuchsin) and heated at 95 °C for 20 min, and 1.2 μL aliquot was loaded on a 6% denaturing polyacrylamide gel containing 6.0 M of urea and electrophoresed using SQ5500-E (HITACHI). For preparation of 500 mL of this gel, 183 g of urea and 60 mL of 50% Long Ranger gel solution (Lonza Rockland, Inc.) were added to ca. 200 mL of water and stirred for 30 min with 6 g of anion and cation exchange resin (AG 501-X8 Resin, Bio-Rad Laboratories, Inc.). After filtration, the resin was rinsed with 60 mL of 10x TBE , and water was added to the filtrate to a 500 mL volume. Electrophoresis was conducted under 1.5 kV, ca. 25 mA, and 40 °C.

Cytotoxicity Assay. The human cancer cell lines tested for cytotoxicities of conjugates **1**−**4** were EBC-1, A549, PC-3, DU145, SK-N-SH, K562. All cells were purchased from Japanese bioresource banks. EBC-1 (JCRB0820, establisher: Hiraki, S.) and A549 (JCRB0076, establisher: Giard, D.) from HSRRB; PC-3, DU145, SK-N-SH, and K562 from RIKEN Cell Bank. EBC-1, A549, and DU145 were cultured in RPMI-1640 (Sigma). PC-3, SK-N-SH, and K562 were cultured in Dulbecco's modified Eagle's medium (Sigma). Each medium contains 10% heat-inactivated fetal bovine serum (JRH Biosciences), penicillin (100 units/mL), and streptomycin (100 μg/mL) (penicillin−streptomycin mixed solution from Nacalai Tesque). The cells were maintained at 37 °C in humidified atmosphere of 95% air and 5% CO_2. Colorimetric assays using WST-8 (Dojindo) were performed on 96-well plates. A 50 μL amount of each cell suspension was added at a density of 5000 cells/well. PI polyamide conjugates **1**−**4** were dissolved in DMSO, and 50 μL of each solution in the medium (final DMSO concentration was 0.1%) was added. After treatment for 48 h, 10 μL of WST-8 reagent was added to each well and incubated at 37 °C. Absorbance was then measured at 450 and 600 nm using an MPR-A4i microplate reader (Tosoh).

Microarray Analysis. An amount of 4 ×10^5 A549 cells was seeded to a 60 mm dish and treated with each conjugate for 12 h in medium containing 0.1% DMSO or 0.1% DMSO solution of each conjugate. The concentrations of conjugates **1**, **2**, **3**, and **4** were 21, 26, 34, and 100 nM which are IC_{50} values of each conjugate, respectively. RNA was extracted using RNeasy Mini Kit (QIAGEN). 3D-Gene Human Oligo chip 25k (Toray Industries Inc., Tokyo, Japan) was used (25 370 distinct genes). Total RNA was labeled with Cy3 or Cy5 using the Amino Allyl MessageAMP II aRNA Amplification Kit (Applied Biosystems, Carlsbad, CA). The Cy3- or Cy5-labeled aRNA pools and hybridization buffer were combined and hybridized for 16 h. Hybridization signals were scanned using a ScanArray Express Scanner (PerkinElmer) and processed by GenePixPro version 5.0 (Molecular Devices). Detected signals for each gene were normalized by a global normalization method (Cy3/Cy5 ratio median = 1). The top 20 downregulated genes and top 10 upregulated genes were picked up for each conjugate from the excel data given.

Animals and Xenografts. Male BALB/c-*nu*/*nu* (SPF/VAF CAnN.Cg-*Foxn1*^{nu}/CrlCrlj nu/nu) mice weighing 15−22 g (5-week old) were obtained from Charles River Laboratories Japan, Inc. (Kanagawa, Japan) for Kitayama Labes Co., Ltd. (Nagano, Japan). Two human cancer cell lines, A549 (Human Science Research Resources Bank, Osaka, Japan) and DU145 (Riken BRC Cell Bank, Tsukuba, Japan), were transplanted to BALB/c-*nu*/*nu* mice (n = 21) in Kitayama Labes. The xenografts were maintained by serial subcutaneous implantation into the right subaxillary region approximately (3 × 10^6 cells/50 μL/mouse for A549 and 3 × 10^6 cells/100 μL/mouse for DU145). HBSS (Hank's Buffered Salt Solution) and BD Matrigel Basement Membrane Matrix were used for A549 and DU145 implantation.

Preparation of Liposomal Solutions. Liposomes were prepared as follows. Egg yolk phosphatidylcholine (Nacalai Tesque, Kyoto, Japan) and a solution of conjugates **2** or **3** in chloroform were put in a glass tube. The solvent was gently evaporated by rotating with a stream of argon gas, and the residual lipid film was then dried overnight under vacuum. The resulting lipid film containing conjugates **2** or **3** was hydrated with Milli-Q water, vortexed lightly to remove the remaining lipid from the glass tube, and finally sonicated for 2 h with an ultrasonic bath. The final concentrations of lipid and conjugates **2** or **3** were 17 mM and 0.33 mg/mL, respectively. Prepared liposomes were stored at 4 °C until use.

Evaluation of in Vivo Antitumor Activity. Xenograft-animals were transferred to Kyoto Institute of Nutrition and Pathology (Kyoto, Japan). The animals were housed in a set of isolators (ICM-1B; Ishizawa Corporation of Medical Implement, Tsukuba, Japan) at 25 ± 1 °C with a relative humidity of 50 ± 10%, and a ventilation frequency of air was approximately 15 times/h under 12 h illumination cycle (8:00−20:00). All mice were allowed free access to feed (sterilized MF, Oriental Yeast; Tokyo, Japan) and tap water throughout this study. The experimental animals were handled in accordance with the guidelines for animal studies of the Kyoto Institute of Nutrition and Pathology. Xenograft animals of each cell line were assigned to three groups (n = 7−10) according to tumor size. For the animal test using conjugates **2** and **3** without liposome, 20 μL of either DMSO or conjugates **2** or **3** in DMSO at 625 μg/mL were injected into each group intraperitoneally. For the animal test using liposomal conjugate **2** or **3**, 125 μL of either liposomal solution or liposomal conjugates **2** or **3** at 330 μg/mL was intravenously injected into each group; lipid concentration for all the solutions was 17 mM. For both tests, these treatments commenced when the tumor volume reached approx-

imately 40 mm^3 of A549 xenograft and 300 mm^3 of DU145 xenograft, respectively, and the weight and tumor volume of each mouse was measured every other day.

■ ASSOCIATED CONTENT

Supporting Information

(1) A figure of unsuccessful polyamide conjugates; (2) schematic representations of putative mismatch sites for each polyamide conjugate; (3) an expanded list of down-/upregulated genes and a table of name, ensemble gene ID, and description of the genes that appear on the list; (4) hierarchical clustering of genes which were within the top or bottom 800 genes of A549 treated with each polyamide conjugate; (5) pathway analysis and a map of apoptosis mechanisms colored according to the expression levels of related genes; (6) tumor volumes and weights of all nude mice used in this paper. This material is available free of charge via the Internet at http://pubs.acs.org.

■ AUTHOR INFORMATION

Corresponding Author

*Phone: 81-75-753-4002; fax: 81-75-753-3670; e-mail: hs@kuchem.kyoto-u.ac.jp (H.S.). E-mail: bando@kuchem.kyoto-u.ac.jp (T.B.).

Notes

The authors declare no competing financial interest.

■ ACKNOWLEDGMENTS

G. Kashiwazaki is a research fellow of the Japan Society for the Promotion of Science (JSPS) and is supported by Grant-in-Aid for JSPS Fellows. This work is also supported by Core Research for Evolutional Science and Technology (CREST) from Japan Science and Technology Agency, a Grant-in-Aid for Priority Research from the Ministry of Education, Culture, Sports, Science, and Technology, Japan, and Global COE Program from JSPS.

■ ABBREVIATIONS USED

PI, *N*-methylpyrrole−*N*-methylimidazole; bp, base pair; *seco*-CBI, 1-chloromethyl-5-hydroxy-1,2-dihydro-3*H*-benz[*e*]indole; PAGE, polyacrylamide gel electrophoresis; DCC, *N*,*N*′-dicyclohexylcarbodiimide; DIEA, *N*,*N*-diisopropylethylamine; DMF, *N*,*N*-dimethylformamide; Fmoc, 9-fluorenylmethoxycarbonyl; HCTU, 1-[bis(dimethylamino)methylene]-5-chloro-1*H*-benzotriazolium 3-oxide hexafluorophosphate; HOBt, 1-hydroxybenzotriazole; MSNT, 1-(mesitylene-2-sulfonyl)-3-nitro-1*H*-1,2,4-triazole; PyBOP, benzotriazol-1-yloxytris-(pyrrolidino)phosphonium hexafluorophosphate; TFA, trifluoroacetic acid; TIS, triisopropylsilane; HPLC, high performance liquid chromatography; BBC3, Bcl-2-binding component 3; CDKN1A, the cyclin-dependent kinase inhibitor 1; GADD45A, the growth-arrest and DNA-damage-inducible protein GADD45A; EPR, enhanced permeability and retention; ESI-TOFMS, electrospray ionization mass spectrometry

■ REFERENCES

(1) (a) Rajski, S. R.; Williams, R. M. DNA cross-linking agents as antitumor drugs. *Chem. Rev.* **1998**, *98*, 2723−2795. (b) Hurley, L. H. DNA and its associated processes as targets for cancer therapy. *Nat. Rev. Cancer* **2002**, *2*, 188−200.

(2) (a) White, S.; Szewczyk, J. W.; Turner, J. M.; Baird, E. E.; Dervan, P. B. Recognition of the four Watson-Crick base pairs in the DNA minor groove by synthetic ligands. *Nature* **1998**, *391*, 468−471. (b) Dervan, P. B. Molecular recognition of DNA by small molecules. *Bioorg. Med. Chem.* **2001**, *9*, 2215−2235. (c) Dervan, P. B.; Edelson, B. S. Recognition of the DNA minor groove by pyrrole-imidazole polyamides. *Curr. Opin. Struct. Biol.* **2003**, *13*, 284−299. (d) Dervan, P. B.; Doss, R. M.; Marques, M. A. Programmable DNA binding oligomers for control of transcription. *Curr. Med. Chem.: Anti-Cancer Agents* **2005**, *5*, 373−387.

(3) (a) Bando, T.; Sugiyama, H. Synthesis and biological properties of sequence-specific DNA alkylating pyrrole-imidazole polyamides. *Acc. Chem. Res.* **2006**, *39*, 935−944. (b) Sasaki, S.; Bando, T.; Minoshima, M.; Shinohara, K.; Sugiyama, H. Sequence-specific alkylation by Y-shaped and tandem hairpin pyrrole-imidazole polyamides. *Chem.—Eur. J.* **2008**, *14*, 864−870. (c) Kashiwazaki, G.; Bando, T.; Shinohara, K.; Minoshima, M.; Nishijima, S.; Sugiyama, H. Cooperative alkylation of double-strand human telomere repeat sequences by PI polyamides with 11-base-pair recognition based on a heterotrimeric design. *Bioorg. Med. Chem.* **2009**, *17*, 1393−1397. (d) Kashiwazaki, G.; Bando, T.; Shinohara, K.; Minoshima, M.; Kumamoto, H.; Nishijima, S.; Sugiyama, H. Alkylation of a human telomere sequence by heterotrimeric chlorambucil PI polyamide .conjugates. *Bioorg. Med. Chem.* **2010**, *18*, 2887−2893. (e) Minoshima, M.; Chou, J. C.; Lefebvre, S.; Bando, T.; Shinohara, K.; Gottesfeld, J. M.; Sugiyama, H. Potent activity against K562 cells by polyamide-seco-CBI conjugates targeting histone H4 genes. *Bioorg. Med. Chem.* **2010**, *18*, 168−174. (f) Minoshima, M.; Bando, T.; Shinohara, K.; Kashiwazaki, G.; Nishijima, S.; Sugiyama, H. Comparative analysis of DNA alkylation by conjugates between pyrrole-imidazole polyamides and chlorambucil or *seco*-CBI. *Bioorg. Med. Chem.* **2010**, *18*, 1236−1243.

(4) Bando, T.; Sasaki, S.; Minoshima, M.; Dohno, C.; Shinohara, K.; Narita, A.; Sugiyama, H. Efficient DNA alkylation by a pyrrole-imidazole CBI conjugate with an indole linker: sequence-specific alkylation with nine-base-pair recognition. *Bioconjugate Chem.* **2006**, *17*, 715−720.

(5) (a) Boger, D. L.; Ishizaki, T.; Kitos, P. A.; Suntornwat, O. Synthesis of *N*-(*tert*-butyloxycarbonyl)-CBI, CBI, CBI-CDPI$_1$, and CBI-CDPI$_2$: enhanced functional analogues of CC-1065 incorporating the 1,2,9,9a-tetrahydrocyclopropa[*c*]benz[*e*]indol-4-one (CBI) left-hand subunit. *J. Org. Chem.* **1990**, *55*, 5823−5832. (b) Boger, D. L.; Yun, W.; Teegarden, B. R. An improved synthesis of 1,2,9,9a-tetrahydrocyclopropa[*c*]benz[*e*]indol-4-one (CBI): a simplified analogue of the CC-1065 alkylation subunit. *J. Org. Chem.* **1992**, *57*, 2873−2876. (c) Boger, D. L.; McKie, J. A. An efficient synthesis of 1,2,9,9a-tetrahydrocyclopropa[*c*]benz[*e*]indol-4-one (CBI): an enhanced and simplified analogue of the CC-1065 and duocarmycin alkylation subunits. *J. Org. Chem.* **1995**, *60*, 1271−1275. (d) Kastrinsky, D. B.; Boger, D. L. Effective asymmetric synthesis of 1,2,9,9a-tetrahydrocyclopropa[*c*]benz[*e*]indol-4-one (CBI). *J. Org. Chem.* **2004**, *69*, 2284−2289.

(6) Shinohara, K.; Bando, T.; Sasaki, S.; Sakakibara, Y.; Minoshima, M.; Sugiyama, H. Antitumor activity of sequence-specific alkylating agents: pyrrole-imidazole CBI conjugates with indole linker. *Cancer Sci.* **2006**, *97*, 219−225.

(7) Bando, T.; Iida, H.; Tao, Z.-F.; Narita, A.; Fukuda, N.; Yamori, T.; Sugiyama, H. Sequence specificity, reactivity, and antitumor activity of DNA-alkylating pyrrole-imidazole diamides. *Chem. Biol.* **2003**, *10*, 751−758.

(8) Dudouet, B.; Burnett, R.; Dickinson, L. A.; Wood, M. R.; Melander, C.; Belitsky, J. M.; Edelson, B.; Wurtz, N.; Briehn, C.; Dervan, P. B.; Gottesfeld, J. M. Accessibility of nuclear chromatin by DNA binding polyamides. *Chem. Biol.* **2003**, *10*, 859−867.

(9) Dickinson, L. A.; Burnett, R.; Melander, C.; Edelson, B. S.; Arora, P. S.; Dervan, P. B.; Gottesfeld, J. M. Arresting cancer proliferation by small-molecule gene regulation. *Chem. Biol.* **2004**, *11*, 1583−1594.

(10) Bando, T.; Narita, A.; Iwai, A.; Kihara, K.; Sugiyama, H. C-H to N substitution dramatically alters the sequence-specific DNA alkylation, cytotoxicity, and expression of human cancer cell lines. *J. Am. Chem. Soc.* **2004**, *126*, 3406−3407.

(11) Burnett, R.; Melander, C.; Puckett, J. W.; Son, L. S.; Wells, R. D.; Dervan, P. B.; Gottesfeld, J. M. DNA sequence-specific polyamides alleviate transcription inhibition associated with long GAA•TTC repeats in Friedreich's ataxia. *Proc. Natl. Acad. Sci. U.S.A.* **2006**, *103*, 11497−11502.
(12) Matsuda, H.; Fukuda, N.; Ueno, T.; Katakawa, M.; Wang, X.; Watanabe, T.; Matsui, S.; Aoyama, T.; Saito, K.; Bando, T.; Matsumoto, Y.; Nagase, H.; Matsumoto, K.; Sugiyama, H. Transcriptional inhibition of progressive renal disease by gene silencing pyrrole-imidazole polyamide targeting of the transforming growth factor-β1 promoter. *Kidney Int.* **2011**, *79*, 46−56.
(13) (a) Chou, C. J.; Farkas, M. E.; Tsai, S. M.; Alvarez, D.; Dervan, P. B.; Gottesfeld, J. M. Small molecules targeting histone H4 as potential therapeutics for chronic myelogenous leukemia. *Mol. Cancer Ther.* **2008**, *7*, 769−778. (b) Chou, C. J.; O'Hare, T; Lefebvre, S.; Alvarez, D.; Tyner, J. W.; Eide, C. A.; Brian, J. D.; Gottesfeld, J. M. Growth arrest of BCR-ABL positive cells with a sequence-specific polyamide-chlorambucil conjugate. *PLoS ONE* **2008**, *3*, e3593.
(14) Harki, D. A.; Satyamurthy, N.; Stout, D. B.; Phelps, M. E.; Dervan, P. B. *In vivo* imaging of pyrrole-imidazole polyamides with positron emission tomography. *Proc. Natl. Acad. Sci. U.S.A.* **2008**, *105*, 13039−13044.
(15) Wang, X.; Nagase, H.; Watanabe, T.; Nobusue, H.; Suzuki, T.; Asami, Y.; Shinojima, Y.; Kawashima, H.; Takagi, K.; Mishra, R.; Igarashi, J.; Kimura, M.; Takayama, T.; Fukuda, N.; Sugiyama, H. Inhibition of MMP-9 transcription and suppression of tumor metastasis by pyrrole-imidazole polyamide. *Cancer Sci.* **2010**, *101*, 759−766.
(16) Chen, M.; Matsuda, H.; Wang, L.; Watanabe, T.; Kimura, M. T.; Igarashi, J.; Wang, X.; Sakimoto, T.; Fukuda, N.; Sawa, M.; Nagase, H. Pretranscriptional regulation of Tgf-β1 by PI polyamide prevents scarring and accelerates wound healing of the cornea after exposure to alkali. *Mol. Ther.* **2010**, *18*, 519−527.
(17) Kupchinsky, S.; Centioni, S.; Howard, T.; Trzupek, J.; Roller, S.; Carnahan, V.; Townes, H.; Purnell, B.; Price, C.; Handl, H.; Summerville, K.; Johnson, K.; Toth, J.; Hudson, S.; Kiakos, K.; Hartley, J. A.; Lee, M. A novel class of achiral *seco*-analogs of CC-1065 and the duocarmycins: design, synthesis, DNA binding, and anticancer properties. *Bioorg. Med. Chem.* **2004**, *12*, 6221−6236.
(18) Sarkar, F. H.; Li, Y.; Wang, Z.; Padhye, S. Lesson learned from nature for the development of novel-anti-cancer agents: implication of isoflavone, curcumin, and their synthetic analogs. *Curr. Pharm. Des.* **2010**, *16*, 1801−1812.
(19) (a) Kaneda, M.; Nomura, S. M.; Ichinose, S.; Kondo, S.; Nakahama, K.; Akiyoshi, K.; Morita, I. Direct formation of proteo-liposomes by *in vitro* synthesis and cellular cytosolic delivery with connexin-expressing liposomes. *Biomaterials* **2009**, *30*, 3971−3977. (b) Moritani, Y.; Nomura, S. M.; Morita, I.; Akiyoshi, K. Direct integration of cell-free-synthesized connexin-43 into liposomes and hemichannel formation. *FEBS J.* **2010**, *277*, 3343−3352.
(20) Maeda, H.; Bharate, G. Y.; Daruwalla, J. Polymeric drugs for efficient tumor-targeted drug delivery based on EPR-effect. *Eur. J. Pharm. Biopharm.* **2009**, *71*, 409−419.
(21) Bando, T.; Narita, A.; Asada, K.; Ayame, H.; Sugiyama, H. Enantioselective DNA alkylation by a pyrrole-imidazole *S*-CBI conjugate. *J. Am. Chem. Soc.* **2004**, *126*, 8948.
(22) (a) Minoshima, M.; Bando, T.; Sasaki, S.; Shinohara, K.; Shimizu, T.; Fujimoto, J.; Sugiyama, H. DNA alkylation by pyrrole-imidazole *seco*-CBI conjugates with an indole linker: sequence-specific DNA alkylation with 10-base-pair recognition through heterodimer formation. *J. Am. Chem. Soc.* **2007**, *129*, 5384−5390. (b) Sasaki, S.; Bando, T.; Minoshima, M.; Shimizu, T.; Shinohara, K.; Takaoka, T.; Sugiyama, H. Sequence-specific alkylation of double-strand human telomere repeat sequence by pyrrole-imidazole polyamides with indole linkers. *J. Am. Chem. Soc.* **2006**, *128*, 12162−12168.